External Validation of the Briganti Nomogram Predicting Lymph Node Invasion in Patients with Intermediate and High-risk Prostate Cancer Diagnosed with Magnetic Resonance Imaging-Targeted and Systematic Biopsies: A European Multicenter Study

Romain Diamand [1], Marco Oderda [2], Simone Albisinni [1], Alexandre Fourcade [3], Georges Fournier [3], Daniel Benamran [4], Christophe Iselin [4], Gaelle Fiard [5], Jean-Luc Descotes [5], Grégoire Assenmacher [6], Ilyas Svistakov [6], Alexandre Peltier [6], Giuseppe Simone [7], Giacomo Di Cosmo [8], Jean-Baptiste Roche [8], Jean-Louis Bonnal [9], Julien Van Damme [10], Maxime Rossi [11], Eric Mandron [11], Paolo Gontero [2] and Thierry Roumeguère [1]

[1] Urology Department, Hôpital Erasme, University Clinics of Brussels, Université Libre de Bruxelles, Brussels, Belgium

[2] Urology Department, Città della Salute e della Scienza di Torino, University of Turin, Turin, Italy

[3] Urology Department, Hôpital Cavale Blanche, CHRU Brest, Brest, France

[4] Urology Department, Hôpitaux Universitaires de Genève, Geneva, Switzerland

[5] Urology Department, CHU de Grenoble, Grenoble, France

[6] Urology Department, Jules Bordet Institute, Brussels, Belgium

[7] Urology Department, Regina Elena National Cancer Institute, Rome, Italy

[8] Urology Department, Clinique Saint-Augustin, Bordeaux, France

[9] Urology Department, Hôpital Saint-Philibert, GHICL, Lille, France

[10] Urology Department, University Clinics Saint-Luc, Université Catholique de Louvain, Brussels, Belgium

[11] Urology Department, Clinique du Pré, Le Mans, France

Corresponding Author
Romain Diamand, MD
University Clinics of Brussels
Erasme Hospital, Urology Department
Route de Lennik 808
1070 Brussels, Belgium
Tel/Fax: +32(2) 555 36 14/99
Email: romain.diamand@erasme.ulb.ac.be

Wordcount
Abstract 251
Manuscript 2384

Keywords
prostate cancer, targeted biopsy, MRI, lymph node invasion, nomogram

Abstract

OBJECTIVE: To validate a nomogram predicting lymph node invasion (LNI) in prostate cancer (PCa) patients undergoing radical prostatectomy (RP) taking into consideration multiparametric-magnetic resonance imaging (mp-MRI) parameters and targeted biopsies in a western European cohort

PATIENTS AND METHODS: A total of 473 men diagnosed by targeted biopsies, using software-based MRI-ultrasound image fusion system, and operated by RP with extended pelvic lymph node dissection (ePLND) across 11 Europeans centers between 2012 and 2019 were identified. Area under the curve (AUC) of the receiver operator characteristic curve (ROC), calibration plot and decision curve analysis (DCA) were used to evaluated the performance of the model

RESULTS: Overall, 56 (11.8%) patients had LNI on final pathologic examination with a median (IQR) of 13 (9-18) resected nodes. Significant differences (all $p<0.05$) were found between patients with and without LNI in terms of preoperative PSA, clinical stage at DRE and mp-MRI, maximum diameter of the index lesion, PI-RADS score, Grade Group on systematic and targeted biopsies, total number of dissected lymph nodes, final pathologic staging and Grade Group. External validation of the prediction model showed a good accuracy with an AUC calculated as 0.8 (CI 95% 0.75-0.86). Graphic analysis of calibration plot and DCA showed a slight underestimation for predictive probability for LNI between 3% and 22% and a high net benefit. A cut-off at 7% was associated with a risk of missing LNI in 2.6%, avoiding unnecessary surgeries in 55.9%

CONCLUSIONS: We report an external validation of the nomogram predicting LNI in patients treated with ePLND in a western European cohort and a cut-off at 7% seems appropriate

Introduction

Extended pelvic lymph node dissection (ePLND) is the most precise method of detecting lymph node invasion (LNI) and has a role in initial staging and prognosis of patients harboring localized prostate cancer (PCa) (1)(2). However, ePLND entails significant morbidity and increases operational time, with complications in up to 20% of patients (1)(3)(4). New imaging modalities are currently being investigated in the initial pre-operative staging, such as ^{68}Ga-PSMA PET/CT or whole-body MRI, with favorable detection and accuracy rates, although their clinical impact remains to be defined and hence are not yet part of the guidelines (5). Abdominal CT scan remains the standard of care, albeit a low sensitivity of around 40% (6).

ePLND is recommended only in patients classified as intermediate- and high-risk PCa, after evaluation of the risk of LNI via available nomograms (2). Several models have been published and regularly updated, such as the Memorial Sloan Kettering Cancer Center (MSKCC) and the Briganti nomogram, taking in consideration mainly clinical parameters (7)(8). These nomograms have been externally validated and the Briganti 2012 nomogram remains the most applied in Europe given its simplicity and applicability to European men. This nomogram exhibits an elevated accuracy when compared to other nomograms (9). A 5% cut-off is usually advised to prompt ePLND at the time of radical prostatectomy, although this value is debated and can be modified with a consequent modification of negative and positive predictive values (2)(8). Furthermore, these nomograms have been developed before the era of multiparametric-MRI (mp-MRI) and targeted biopsies. In this context, a novel model, the Briganti 2019 nomogram, has been published adding new parameters such as Gleason score (ISUP Grade Group, Supplementary Table 1) on targeted biopsies and clinical staging by mp-MRI with the assumption that the previous models might be suboptimal in term of performance

when applied to contemporary patients. This resulted in an improvement of accuracy and net clinical benefit when compared to Briganti 2012-2017 and MSKCC nomograms (10).

Aim of the current research was to perform an external validation of the Briganti 2019 nomogram using a multicentric western European cohort.

Materials and Methods

After obtaining institutional review boards approval, data has been retrospectively gathered on 545 radical prostatectomies and ePLND patients across 11 Europeans centers (Belgium, France, Switzerland and Italy). All patients had undergone preoperative mp-MRI and elastic software-based MRI-ultrasound image fusion targeted and systematic biopsies using the KOELIS system (KOELIS, La Tronche, France) between March 2012 and January 2019. We excluded 72 patients from final analysis given incomplete data to perform the nomogram.

All men underwent mp-MRI 1.5 or 3T with or without endorectal coil. Mp-MRI protocol respected the European Society of Urogenital Radiology guidelines using T1- and T2-weighted, Diffusion-Weighted Imaging (DWI) and Dynamic Contrast Enhancement (DCE) (11). All exams were read by a dedicated uro-radiologist using the Prostate Imaging-Reporting and Data System (PI-RADS) protocol (11). Targeted biopsies were then performed if PI-RADS score was ≥ 3 using exclusively the KOELIS system (Trinity® or Touch®). These devices allow a reconstruction of prostatic 3D anatomy after elastic fusion of MRI images and 3D ultrasound (US), associated to Organ-Based Tracking® to enhance precision (12). In the present study, median (IQR) number of biopsy cores was 12 (12-13) and 4 (3-6) for systematic and targeted biopsies respectively.

The indication for surgical intervention was decided by the treating urologist after a clinical encounter. No patient received neoadjuvant therapy nor hormonal treatment in the 12 months preceding surgery. ePLND was performed during surgery, including the same lymph node template in all patients. Lymph nodes dissected included ileo-obturator, external iliac, hypogastric, and common iliac LNs limited superiorly by the ureter crossing. A dedicated pathologist, the same who analyzed the biopsy specimens, was in charge for the pathologic examination of prostatectomy and ePLND in each center.

Examined variables were recorded both in preoperative and post-operative setting. These included preoperative PSA, clinical stage based on digital rectal examination (cT), number of suspected lesions on mp-MRI, PI-RADS score, maximal diameter of lesion on mp-MRI (defined as the largest diameter on any axis of the index lesion), extracapsular extension and seminal vesicle invasion at mp-MRI ($_{i}$cT). Moreover, number of positive biopsies and Grade Groups on biopsies were examined (13). Post-operative data included final Grade Groups, pathologic staging, total number of resected lymph nodes, number of positive nodes and peri- and post-operative complications. Data were described using frequency for categorical data, and median with interquartile range for continuous data exhibiting a non-parametrical distribution. Mann-Whitney test and χ^2 test were used as appropriate to compare medians and frequencies, respectively.

External validation followed the TRIPOD recommendations (14). First, we evaluated the performance of the Briganti 2012 nomogram (7). Given the absence of distinction between targeted and systematic biopsies in this nomogram, we merged the two biopsies techniques to calculate the probability for LNI. Then, we validated and evaluated the performance of the Briganti 2019 nomogram (10). Previously published regression coefficients for each parameter were used to calculate the individual risk of LNI (Supplementary Table 2). Performance of the model was evaluated in terms of discrimination and calibration. Discrimination was quantified

using the area under the curve (AUC) from the receiver operated characteristic curve (ROC). The extent of over- and underestimation associated with the model was graphically described using calibration plots. Decision curve analysis (DCA) was used to evaluate the net benefice of the model according to the cut-off (15). A two-sided $p<0.05$ defined statistical significance. All statistical analysis were performed with STATA 14.1 (StataCorp, Texas, USA).

Results

The characteristics of the patient cohort are presented in Table 1. Overall, 56 (11.8%) patients had LNI on final pathologic examination with a median (IQR) of 13 (9-18) resected nodes. Significant differences (all $p<0.05$) were found across pN0 and pN1 patients regarding preoperative PSA, cT and $_{i}$cT, PI-RADS score, maximal diameter of the index lesion, number of positive biopsies, Grade Groups on systematic and targeted biopsies, final pathologic staging and Grade Groups, positive margins and total number of dissected lymph nodes.

The AUC of Briganti 2012 was evaluated at 0.8 (CI 95% 0.74-0.87). Graphical analysis of calibration plots was satisfactory with a general tendency to underestimation (Supplementary Fig.1). Regarding the Briganti 2019 nomogram, Figure 1 illustrates the ROC curve with an AUC calculated as 0.8 (CI 95% 0.75-0.86). Graphic representation of calibration is presented in Figure 2. An overall slight underestimation can be observed for predictive probability for LNI between 3% and 22%. The DCA demonstrates that the 2019 model improved clinical risk prediction against threshold probabilities of LNI $\leq$ 20% (Figure 3). However, we note that the net benefit for the Briganti 2019 was higher than the 2012 model for threshold probabilities below 10%.

Table 2 shows the proportion of missing LNI according to the cut-off decided to perform ePLND. Considering values of 5% and 7%, 195 (46.4%) and 235 (55.9%) patients would have avoided an ePLND with a total of 4 (2.1%) and 6 (2.6%) men harboring LNI which would have been missed respectively.

A total of 8 (2.2%) per-operative complications were described with a majority of intraoperative bowel injuries treated intraoperatively with no consequences. Regarding post-operative complications, 58 (15.6%) were described with 20 (5.4%) grade ≥ III according to Clavien-Dindo classification. A majority of lymphoceles were observed in 20 patients (5.4%) requiring percutaneous drainage in 6 patients (1.6%) (Supplementary Table 3).

Discussion

The aim of the current study was to externally validate the predictive model of Briganti 2019 using a cohort of 473 men from several European centers and an AUC of 0.8 was reported. These results are slightly less optimistic compared to the internal validation which yielded an AUC of 0.86, although remaining favorable and validating the nomogram.

The proportion of LNI described on final pathology and sample size was globally similar across the two external and internal validation cohorts (11.8% vs. 12.5% for LNI and 473 vs. 497 men, respectively). Nonetheless, several apparent differences had to be underlined regarding important variables such as predictors and outcomes. In our cohort we described a higher proportion of lesion with PI-RADS score 5 (45% vs. 22.3%, p<0.0001), differences in terms of Grade Groups at targeted biopsy (32.3% vs. 48.3% for Grade Group 2 respectively, p<0.0001, and 24.1% vs. 17.7% for Grade Group 3 respectively, p=0.02), larger MRI index lesions described on mp-MRI (13mm vs. 10mm for pN0 and 20mm vs. 15mm for pN1respectively) and more localized disease on final pathology examination (61.7% vs. 42.2%

for pT2, $p<0.0001$). These differences can explain the variation in precision across the internal validation and the present study. As such, this nomogram can be applied to the western European population, maintaining valid discriminatory characteristics, although variations according to the threshold will be inevitable. As such, the clinician's judgment remains capital in deciding the optimal cut-off for his particular practice.

We also evaluated the Briganti 2012 nomogram, which remains probably the most used in Europe (9). Although in our cohort the precision was similar to the new model (AUC of 0.8) with a comparable 95% confidence interval, we found that the Briganti 2019 model had the best clinical value with highest net benefit for threshold probabilities under 10%. Moreover, given the introduction of mp-MRI and targeted biopsies in current clinical practice, we recommend to implement the new Briganti 2019 nomogram, allowing a correct interpretation of clinical data and avoiding confusion (clinical vs. MRI stage, targeted vs. systematic biopsies). Indeed, models were previously developed with only systematic biopsies. Moreover, lower stages and lower grades diseases were more frequently operated given the absence of well-structured active surveillance programs (16)(17). The introduction of mp-MRI in clinical practice allows a better definition of local staging, adding information of lesion localization, size and eventual extracapsular extension and seminal vesicle invasion. Mp-MRI has thus opened the door to targeted biopsies, with an improvement of diagnostic performance and a better detection for significant PCa, as well as histologic concordance with final pathology (18)(19)(20)(21). As such, this new nomogram reflects the evolution of the diagnostic pathway of PCa patients.

In the present study we found a median (IQR) of 13 (9-18) resected lymph nodes, with an 11.8% of pN1, which is relatively close to the values published by Gandaglia et al. with 15 (11-20) resected lymph nodes and 12.5% of pN1 (10). In a systematic review of literature, Fossati et al. reported a median of 4-28 resected nodes for ePLND associated to 3.3%-26.2% of pN1 (1). This large variability can be explained by multiple factors, including surgical

technique and pathologic manipulation of the specimen, as well as definition of the boundaries of ePLND which included common iliac and presacral space for some studies (22). Fossati et al. in collaboration with the EAU PCa Guidelines panel have now proposed limits for ePLND, not including common iliac and presacral nodes (1). Finally, the absolute number of nodes does not define the type of dissection. It is rather the anatomic template which remains the most significant element in defining the type of dissection. As a confirmation, Weingartner et al. performed cadaveric dissections, yielding high variation from 8 to 56 lymph nodes in templates of ePLND (23)(24). Furthermore, it should be highlighted that there is no consensus for the pathologic identification, analysis and count of lymph nodes on pathologic examination (25).

We described 15.6% post-operative complications, mainly lymphoceles (5.4%) not requiring specific treatment. This is in accordance with data described in a systematic review by Ploussard et al., with 0-7.9% of symptomatic lymphoceles after ePLND (3). We also observed severe complications directly related to lymph node dissection required reintervention such as massive lymphocele or ureteral lesion requiring reimplantation. The morbidity associated to ePLND includes longer operative time and hospital stay with a consequent impact on healthcare budgets. As such, a precise selection of candidate for ePLND is crucial and using a nomogram could avoid extended surgery.

If we implemented a cut-off of 5% or 7%, the proportion of patients harboring LNI missed would have remained < 3% (46.4% and 55.9% of patients would have avoided an ePLND with a consequent miss of 2.1% and 2.6%, respectively), which is only slightly higher to that reported by Gandaglia et al. (51% and 57% avoiding ePLND with missing LNI in 1.8% and 1.5% for a cut-off of 5% and 7%, respectively) (10). European recommendations apply a 5% cut-off, based on the Briganti 2012 study, while NCCN recommend rather 2% based on the MSKCC model (2)(26). This arbitrary cut-off should be interpreted with caution by the clinician in order to perform ePLND in the correct patients and avoid unnecessary surgeries and

complications. Recently, a cut-off at 7% has been proposed in order to reduce redundant interventions, which seems reasonable in light of our results (8)(10). However, as showed by the calibration plot, an underestimation is possible at low prediction value, therefore putting the clinician at risk of defining a higher "real life" risk compared to the predicted value.

Our study is not devoid of limitations. First, the cohort is multicentric, all centers adhered to the guidelines and terminology in current practice but with a consequent heterogeneity in mp-MRI reporting, biopsy analysis and surgery technique due to the implication of multiple physicians with different spectrum of expertise. Targeted biopsies were all performed by KOELIS system, reducing subjectivity and variability compared to cognitive approach (27)(28). Despite the absence of central pathologic reviewing, the same pathologist interpreted biopsies and final pathologic specimens in every center to reduce bias. Second, the sample size and number of events were relatively small. Almost 71% of patients were recruited during the last two years which could be explained by recent evidence about the benefit of targeted biopsy in the diagnosis of prostate cancer (18)(29). Third, our population included only operated patients; hence care must be taken when using the nomogram for other therapeutic modalities such as radiotherapy, focal therapy or active surveillance. Finally, the retrospective nature of the study limits the interpretation of data, as it inevitably introduced selection bias.

Conclusions

We herein report an external validation of the new Briganti 2019 nomogram predicting LNI. The model presents a good performance with an AUC of 0.8. Based on these results, this nomogram could be applied in the western European population and a cut-off at 7% seems appropriate with a risk of missing LNI in 2.6% and avoiding unnecessary surgeries in 55.9%.

Further prospective studies are needed to define the role of ePLND in the surgical management of PCa.

Disclosure of Potential Conflicts of Interest

All the authors have nothing to disclose.

References

1. Fossati N, Willemse PPM, Van den Broeck T, van den Bergh RCN, Yuan CY, Briers E, et al. The Benefits and Harms of Different Extents of Lymph Node Dissection During Radical Prostatectomy for Prostate Cancer: A Systematic Review. European Urology. 2017.
2. Mottet N, Bellmunt J, Bolla M, Briers E, Cumberbatch MG, De Santis M, et al. EAU-ESTRO-SIOG Guidelines on Prostate Cancer. Part 1: Screening, Diagnosis, and Local Treatment with Curative Intent. Eur Urol. 2017.
3. Ploussard G, Briganti A, De La Taille A, Haese A, Heidenreich A, Menon M, et al. Pelvic lymph node dissection during robot-assisted radical prostatectomy: Efficacy, limitations, and complications - A systematic review of the literature. European Urology. 2014.
4. Briganti A, Chun FKH, Salonia A, Suardi N, Gallina A, Da Pozzo LF, et al. Complications and Other Surgical Outcomes Associated with Extended Pelvic Lymphadenectomy in Men with Localized Prostate Cancer. Eur Urol. 2006.
5. Esen T, Kılıç M, Seymen H, Acar Ö, Demirkol MO. Can Ga-68 PSMA PET/CT replace conventional imaging modalities for primary lymph node and bone staging of prostate cancer? European Urology Focus. 2019.
6. Hövels AM, Heesakkers RAM, Adang EM, Jager GJ, Strum S, Hoogeveen YL, et al. The diagnostic accuracy of CT and MRI in the staging of pelvic lymph nodes in patients with prostate cancer: a meta-analysis. Clin Radiol. 2008.
7. Briganti A, Larcher A, Abdollah F, Capitanio U, Gallina A, Suardi N, et al. Updated nomogram predicting lymph node invasion in patients with prostate cancer undergoing extended pelvic lymph node dissection: The essential importance of percentage of positive cores. Eur Urol. 2012.
8. Gandaglia G, Fossati N, Zaffuto E, Bandini M, Dell'Oglio P, Bravi CA, et al. Development and Internal Validation of a Novel Model to Identify the Candidates for Extended Pelvic Lymph Node Dissection in Prostate Cancer. Eur Urol. 2017.

9. Hueting TA, Cornel EB, Somford DM, Jansen H, van Basten JPA, Pleijhuis RG, et al. External Validation of Models Predicting the Probability of Lymph Node Involvement in Prostate Cancer Patients. Eur Urol Oncol. 2018.

10. Gandaglia G, Ploussard G, Valerio M, Mattei A, Fiori C, Fossati N, et al. A Novel Nomogram to Identify Candidates for Extended Pelvic Lymph Node Dissection Among Patients with Clinically Localized Prostate Cancer Diagnosed with Magnetic Resonance Imaging-targeted and Systematic Biopsies. Eur Urol. 2019.

11. Padhani AR, Weinreb J, Rosenkrantz AB, Villeirs G, Turkbey B, Barentsz J. Prostate Imaging-Reporting and Data System Steering Committee: PI-RADS v2 Status Update and Future Directions. Eur Urol. 2019.

12. Baco E, Ukimura O, Rud E, Vlatkovic L, Svindland A, Aron M, et al. Magnetic resonance imaging-transectal ultrasound image-fusion biopsies accurately characterize the index tumor: Correlation with step-sectioned radical prostatectomy specimens in 135 patients. Eur Urol. 2015.

13. Epstein JI, Egevad L, Amin MB, Delahunt B, Srigley JR, Humphrey PA. The 2014 international society of urological pathology (ISUP) consensus conference on gleason grading of prostatic carcinoma definition of grading patterns and proposal for a new grading system. Am J Surg Pathol. 2016.

14. Collins GS, Reitsma JB, Altman DG, Moons KGM. Transparent reporting of a multivariable prediction model for individual prognosis or diagnosis (TRIPOD): The TRIPOD Statement. Eur Urol. 2015.

15. Vickers AJ, Van Calster B, Steyerberg EW. Net benefit approaches to the evaluation of prediction models, molecular markers, and diagnostic tests. BMJ. 2016.

16. van den Bergh R, Gandaglia G, Tilki D, Borgmann H, Ost P, Surcel C, et al. Trends in Radical Prostatectomy Risk Group Distribution in a European Multicenter Analysis of 28 572 Patients: Towards Tailored Treatment. Eur Urol Focus. 2019.

17. Albisinni S, Joniau S, Quackels T, De Coster G, Dekuyper P, Van Cleynenbreugel B, et al. Current trends in patient enrollment for robotic-assisted laparoscopic prostatectomy in Belgium. Cancer. 2017.

18. Kasivisvanathan V, Rannikko AS, Borghi M, Panebianco V, Mynderse LA, Vaarala MH, et al. MRI-targeted or standard biopsy for prostate-cancer diagnosis. N Engl J Med. 2018.

19. van der Leest M, Cornel E, Israël B, Hendriks R, Padhani AR, Hoogenboom M, et al. Head-to-head Comparison of Transrectal Ultrasound-guided Prostate Biopsy Versus Multiparametric Prostate Resonance Imaging with Subsequent Magnetic Resonance-guided Biopsy in Biopsy-naïve Men with Elevated Prostate-specific Antigen: A Large Prospective Mu. Eur Urol. 2019.

20. Diamand R, Oderda M, Al Hajj Obeid W, Albisinni S, Van Velthoven R, Fasolis G, et al. A multicentric study on accurate grading of prostate cancer with systematic and MRI/US fusion targeted biopsies: comparison with final histopathology after radical prostatectomy. World J Urol. 2019.

21. Cornud F, Roumiguié M, De Longchamps NB, Ploussard G, Bruguière E, Portalez D,

et al. Precision matters in MR imaging-targeted Prostate biopsies: Evidence from a prospective study of cognitive and elastic fusion registration transrectal biopsies. Radiology. 2018.

22. Heidenreich A, Varga Z, Von Knobloch R. Extended pelvic lymphadenectomy in patients undergoing radical prostatectomy: High incidence of lymph node metastasis. J Urol. 2002.

23. Weingärtner K, Ramaswamy A, Bittinger A, Gerharz EW, Vöge D, Riedmiller H. Anatomical basis for pelvic lymphadenectomy in prostate cancer: Results of an autopsy study and implications for the clinic. J Urol. 1996.

24. Heidenreich A, Pfister D. Pelvic lymphadenectomy in clinically localised prostate cancer: Counting lymph nodes or dissecting primary landing zones of the prostate? European Urology. 2014.

25. Prendeville S, Berney DM, Bubendorf L, Compérat E, Egevad L, Hes O, et al. Handling and reporting of pelvic lymphadenectomy specimens in prostate and bladder cancer: a web-based survey by the European Network of Uropathology. Histopathology. 2019.

26. Mohler JL, Antonarakis ES, Armstrong AJ, D'Amico A V., Davis BJ, Dorff T, et al. Prostate Cancer, Version 2.2019, NCCN Clinical Practice Guidelines in Oncology. J Natl Compr Canc Netw. 2019.

27. Cool DW, Zhang X, Romagnoli C, Izawa JI, Romano WM, Fenster A. Evaluation of MRI-TRUS fusion versus cognitive registration accuracy for MRI-targeted, TRUS-guided prostate biopsy. Vol. 204, American Journal of Roentgenology. 2015.

28. Wegelin O, van Melick HHE, Hooft L, Bosch JLHR, Reitsma HB, Barentsz JO, et al. Comparing Three Different Techniques for Magnetic Resonance Imaging-targeted Prostate Biopsies: A Systematic Review of In-bore versus Magnetic Resonance Imaging-transrectal Ultrasound fusion versus Cognitive Registration. Is There a Preferred Technique? Vol. 71, European Urology. 2017.

29. Ahmed HU, El-Shater Bosaily A, Brown LC, Gabe R, Kaplan R, Parmar MK, et al. Diagnostic accuracy of multi-parametric MRI and TRUS biopsy in prostate cancer (PROMIS): a paired validating confirmatory study. Lancet. 2017.

Table 1. Descriptive perioperative characteristics of the external validation cohort with comparison between the group with negative and positive lymph nodes

		Overall	pN0	pN1	p^b
Patient, *n* (%)		473 (100)	417 (88.2)	56 (11.8)	
Median age at surgery, yr (IQR)		66 (62-71)	66 (62-71)	66 (63-69)	0.7
Median BMI, kg/m^2 (IQR)		26.3 (23.8-28.8)	26.3 (23.9-28.8)	28 (25.2-30.9)	0.4
Median preoperative PSA, ng/ml (IQR)		8 (5-11.1)	8 (5.1-11)	10.1 (8.4-14.3)	0.02
Clinical stage at DRE, *n* (%)					
	T1	253 (53.5)	236 (56.6)	17 (30.4)	< 0.0001
	T2	199 (42.1)	164 (39.3)	35 (62.5)	
	T3	7 (1.5)	3 (0.7)	4 (7.1)	
	Unknown	14 (2.9)	14 (3.4)	0 (0)	
No. of suspicious lesions on MRI, *n* (%)					
	1	289 (61.1)	249 (59.7)	40 (71.4)	0.6
	2	124 (26.2)	113 (27.1)	11 (19.6)	
	3	48 (10.1)	43 (10.3)	5 (8.9)	
	≥4	12 (2.5)	12 (2.9)	0 (0)	
PI-RADS score of index lesion, *n* (%)					
	3	40 (8.5)	39 (9.4)	1 (1.8)	< 0.0001
	4	192 (40.6)	182 (43.6)	10 (17.9)	
	5	213 (45)	174 (41.7)	39 (69.6)	
	Unknown	28 (5.9)	22 (5.3)	6 (10.7)	
Median maximum diameter of index lesion, mm (IQR)		14 (10-18)	13 (10-17)	20 (14-26)	< 0.0001
Anterior localization of index lesion, *n* (%)		101 (21.4)	39 (9.4)	10 (17.9)	0.5
Clinical stage on MRI, *n* (%)					
	T2 (organ-confined)	387 (81.8)	351 (84.2)	36 (64.3)	< 0.0001
	T3a (extracapsular extension)	58 (12.3)	50 (12)	8 (14.3)	
	T3b (seminal vesicle invasion)	13 (2.7)	3 (0.7)	10 (17.8)	
	Unknown	15 (3.2)	13 (3.1)	2 (3.6)	
Median no. of cores taken, overall, *n* (IQR)		16 (14-18)	16 (14-18)	16 (14-18)	0.7
Median no. of positive cores, overall, *n* (IQR)		6 (4-9)	6 (4-9)	9 (6-12)	< 0.0001
Median no. of cores with csPCa, overall, *n* (IQR)		3 (4)	3 (3)	6 (5)	< 0.0001
ISUP Grade Group on biopsy, overall, *n* (%)					
	1	50 (10.5)	49 (11.8)	1 (1.8)	< 0.0001
	2	193 (40.8)	181 (43.4)	12 (21.4)	
	3	122 (25.8)	103 (24.7)	19 (33.9)	
	4	75 (15.9)	67 (16.1)	8 (14.3)	
	5	33 (7)	17 (4.1)	16 (28.6)	
Median no. of MRI-targeted cores taken, *n* (IQR)		4 (3-6)	4 (3-6)	4 (3-6)	0.3
Median no. of positive MRI-targeted cores, n (IQR)		3 (2-5)	2 (1-4)	4 (2-6)	< 0.0001
Median no. of MRI-targeted cores with csPCa, *n* (IQR)		2 (1-3)	2 (1-3)	2 (1-3)	< 0.0001
ISUP Grade Group on MRI-targeted biopsy, *n* (%)					
	Negative	48 (10.2)	46 (11.1)	2 (3.5)	< 0.0001
	1	62 (13.1)	60 (14.4)	2 (3.6)	

	2	153 (32.3)	145 (34.8)	8 (14.3)	
	3	114 (24.1)	94 (22.5)	20 (35.7)	
	4	68 (14.4)	59 (14.1)	9 (16.1)	
	5	28 (5.9)	13 (3.1)	15 (26.8)	
Median no. of systematic cores taken, *n* (IQR)		12 (12-13)	12 (12-13)	12 (11-13)	0.8
Median no. of positive systematic cores, overall, *n* (IQR)		3 (1-5)	3 (1-5)	4 (2-6)	0.002
Median no. of systematic cores with csPCa, *n* (IQR)		1 (0-3)	1 (0-3)	2 (0-4)	0.003
ISUP Grade Group on systematic biopsy, *n* (%)					
	Negative	52 (11)	49 (11.8)	3 (5.4)	< 0.0001
	1	87 (18.4)	84 (20.1)	3 (5.4)	
	2	157 (33.2)	143 (34.3)	14 (25)	
	3	93 (19.7)	81 (19.4)	12 (21.4)	
	4	64 (13.5)	52 (12.5)	12 (21.4)	
	5	20 (4.2)	8 (1.9)	12 (21.4)	
Surgical technique, *n* (%)					
	Open RP	23 (4.9)	22 (5.3)	1 (1.8)	0.4
	Laparoscopic RP	71 (15)	64 (15.3)	7 (12.5)	
	Robotic-assisted RP	379 (80.1)	331 (79.4)	48 (85.7)	
ISUP Grade Group on final specimen, *n* (%)					
	1	26 (5.5)	25 (6)	1 (1.8)	< 0.0001
	2	180 (38.1)	171 (41)	9 (16.1)	
	3	168 (35.5)	152 (36.5)	16 (28.6)	
	4	50 (10.6)	43 (10.3)	7 (12.5)	
	5	49 (10.4)	26 (6.2)	23 (41.1)	
Pathologic stage, *n* (%)					
	T2	292 (61.7)	283 (67.9)	9 (16.1)	< 0.0001
	T3a	120 (25.4)	103 (24.7)	17 (30.4)	
	T3b	60 (12.7)	31 (7.4)	29 (51.8)	
	T4	1 (0.2)	0 (0)	1 (1.8)	
Positive surgical margin, *n* (%)		141 (29.8)	110 (26.4)	31 (55.4)	< 0.0001
Median prostate weight, g (IQR)		46 (35-58)	46 (34-57)	49 (36-62)	0.9
Median no. of lymph node removed, *n* (IQR)		13 (9-18)	13 (9-17)	15 (9-22)	0.03
Positive lymph node, *n* (IQR)		0 (0)	-	1 (0-2)	
Intra-operative complication, *n* (%)[a]					
	Overall	8 (2.2)	8 (2.1)	0 (0)	0.4
	Digestive perforation	7 (1.9)	7 (1.9)	-	
	Ureteral perforation	1 (0.3)	1 (0.3)	-	
Post-operative complication, *n* (%)[a]					
	Overall	58 (15.6)	49 (14.8)	9 (2.4)	0.2
	Lymphocele	20 (5.4)	15 (4.5)	5 (1.3)	
	Hematoma	8 (2.2)	7 (2.1)	1 (0.3)	
	Anastomotic leak	7 (1.9)	7 (2.1)	0 (0)	

IQR: interquartile range ; PSA: prostate specific antigen ; BMI: body mass index ; DRE: digital rectal examination ; MRI: magnetic resonance imaging ; PI-RADS: prostate imaging-reporting and data system ; csPCa: clinically significant prostate cancer ; RP: radical prostatectomy ; ISUP: international society of urological pathology ;

[a] Data available for 372 patients

[b] $\chi 2$ and Mann-Whitney tests for categorical and continuous data respectively		

Table 2. Risk of missing LNI according to the cut-off decided to perform ePLND

	No. of patients below the cut-off (ePLND not recommended), *n* (%)			No. of patients above the cut-off (ePLND recommended), *n* (%)			
Cut-off (%)	Total	Without LNI	With LNI	Total	Without LNI	With LNI	NPV (%)
2	47 (11.2)	47 (100)	0 (0)	373 (88.8)	325 (87.1)	48 (12.9)	100
3	143 (34)	141 (98.6)	2 (1.4)	277 (66)	231 (83.4)	46 (16.6)	98.6
4	178 (42.4)	175 (98.3)	3 (1.7)	242 (57.6)	197 (81.4)	45 (18.6)	98.3
5	195 (46.4)	191 (97.9)	4 (2.1)	225 (53.6)	181 (80.4)	44 (19.6)	97.9
6	215 (51.2)	209 (97.2)	6 (2.8)	205 (48.8)	163 (79.5)	42 (20.5)	97.2
7	235 (55.9)	229 (97.4)	6 (2.6)	185 (44.1)	143 (77.3)	42 (22.7)	97.4
8	253 (60.2)	243 (96)	10 (4)	167 (39.8)	129 (77.2)	38 (22.8)	96
9	267 (63.6)	256 (95.9)	11 (4.1)	153 (36.4)	116 (75.8)	37 (24.2)	95.9
10	284 (67.6)	270 (95.1)	14 (4.9)	136 (32.4)	102 (75)	34 (25)	95.1

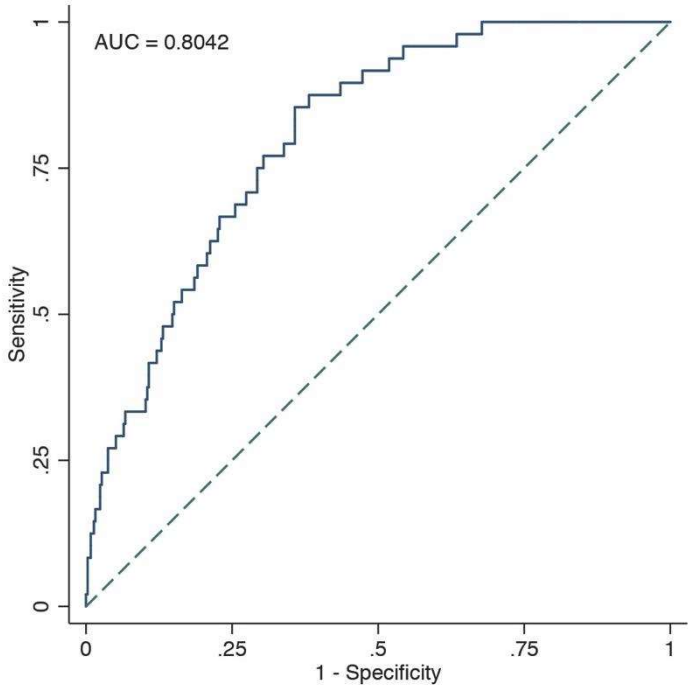

Figure 1. Receiving operator characteristic (ROC) curve for the prediction model

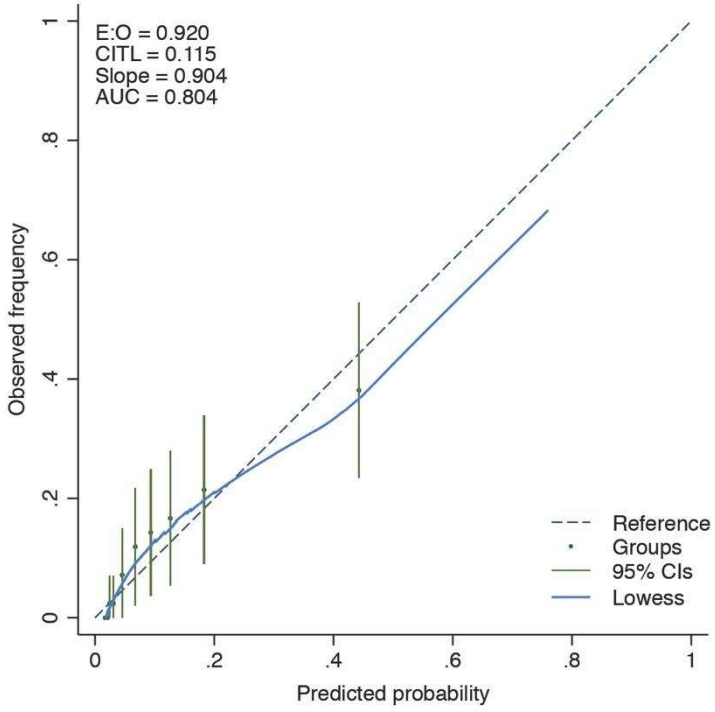

Figure 2. Calibration plot for the prediction model with the overall external validation cohort (intercept=0.1 and slope=0.9). EO: exp/obs ratio ; CITL: calibration-in-the-large ; AUC: area under the curve

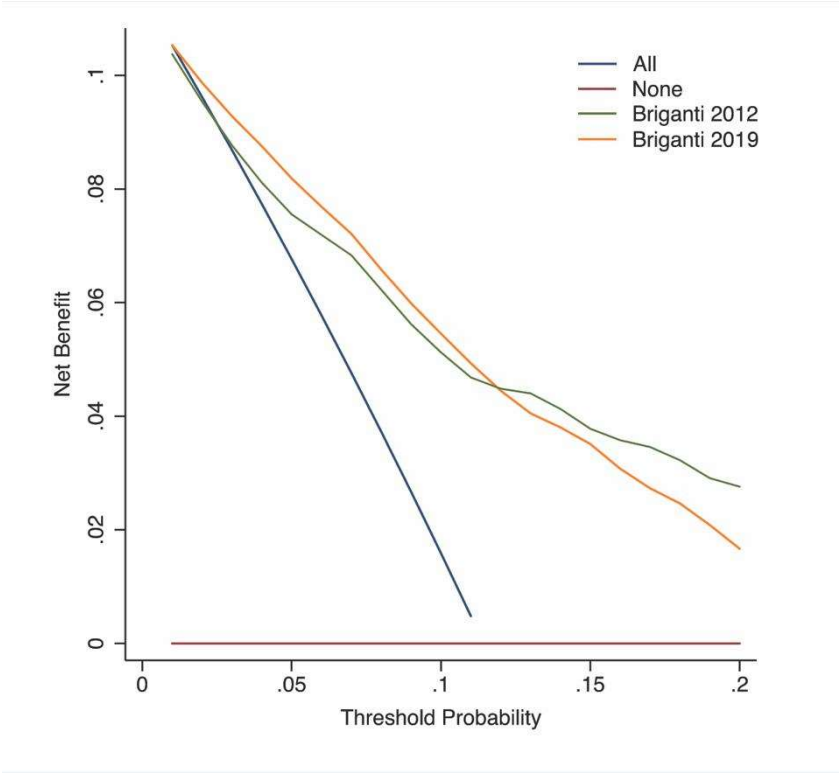

Figure 3. Decision curve analysis (DCA) for the evaluation of the net benefit according to the threshold probability with the use of predictions models